State of Florida

Department of Transportation

CONSTRUCTION OF DYNAMIC MODULUS MASTER CURVES USING RESILIENT MODULUS AND CREEP TEST DATA

FDOT Office

State Materials Office

Research Report Number

FL/DOT/SMO/11-544

Authors

Hyung S. Lee

Sungho Kim

Bouzid Choubane

Date of Publication

July 2011

TABLE OF CONTENTS

LIST OF FIGURES

LIST OF TABLES

1 Executive Summary

For the past few decades, the stiffness of materials used for roadway design and construction has been commonly characterized by the resilient modulus, defined as the ratio of the applied stress to the recoverable strain. However, the resilient modulus is not a fundamental material property of a viscoelastic material, and hence, the concept of resilient modulus has been subsequently diminished in the latest Mechanistic-Empirical Pavement Design Guide (MEPDG). Although the MEPDG could not endorse the use of the resilient modulus test protocol as the primary means of asphalt concrete modulus characterization in the design of flexible pavements, it has been a primary mixture test, and a considerable amount of laboratory testing has been completed to date. In this paper, analysis methodologies are introduced for backcalculating the dynamic modulus from the resilient modulus test data. To assess the usefulness of the proposed algorithm, laboratory experiments in both the uniaxial compression and indirect tensile test modes were carried out on asphalt specimens compacted using the Superpave gyratory compactor. The backcalculated dynamic modulus was used to generate the master curve, and the creep test data was used to enhance the accuracy of the master curve. The advantage of such a methodology is that the existing resilient modulus and creep test data can be leveraged for estimating the dynamic modulus. The approach would significantly save time and effort in reevaluating the dynamic modulus of asphalt mixture when the resilient modulus and creep test data are available.

2 INTRODUCTION

For the past few decades, the resilient modulus defined as the ratio of the applied stress to the recoverable strain (*1*), has been commonly used by highway agencies for characterizing the stiffness of asphalt concrete mixtures. As for the Florida Department of Transportation (FDOT), resilient modulus test has been typically conducted along with creep and strength tests in the Indirect Tensile (IDT) mode for obtaining the Energy Ratio, a single parameter which depicts the relative cracking performance of a mixture based on the theory of Fracture Mechanics (*2*, *3*). Unfortunately, the resilient modulus is not a fundamental property of a viscoelastic material, and hence the concept of resilient modulus has been subsequently diminished in the latest Mechanistic-Empirical Pavement Design Guide (*4*). Instead, the new design guide uses the dynamic modulus as a primary material input for both new construction and rehabilitation projects.

Although the resilient modulus was not adopted for use in the new design guide, a considerable amount of resilient modulus data has been gathered in the past to evaluate asphalt mixtures. On the other hand, because the dynamic modulus test was not needed for the calculation of Energy Ratio, it has not been conducted during most of FDOT's previous research studies. Therefore, there is a need for a reliable and accurate methodology that allows for converting the existing resilient modulus data to dynamic modulus, in order to make use of the existing resilient modulus data along with the new design guide.

In a recent study, Lee and Kim (*5*) proposed a direct methodology for backcalculating the fundamental property of a viscoelastic material from an arbitrary loading function by means of the method of least squares. The authors showed that if the historical resilient modulus test data are available for a given asphalt mixture, then it is possible to backcalculate the dynamic modulus from the test data by treating the resilient modulus loading as the arbitrary loading. The methodology showed promising potential as it was able to backcalculate the dynamic modulus of both laboratory-fabricated and field-cored asphalt specimens from the resilient modulus test data

at multiple temperatures (0°C, 10°C, and 20°C) in the uniaxial compression mode as well as in the indirect tension (IDT) mode.

3 OBJECTIVE AND SCOPE OF WORK

The objective of this study was to construct the master curve of an asphalt mixture from the dynamic modulus values backcalculated from the resilient modulus test data. In addition, the creep test data which FDOT has typically been collecting with the resilient modulus data is introduced to enhance the accuracy of the master curve constructed from the backcalculated modulus.

4 REVIEW OF BACKCALCULATION METHODOLOGY FOR UNIAXIAL TESTING CONDITIONS

In this section, the mathematical formulation of the backcalculation algorithm will be reviewed briefly. Interested readers are referred to Lee and Kim (*5*) for a more detailed derivation.

4.1 Numerical Evaluation of the Convolution Integral

Based on the theory of linear viscoelasticity, the relationship between time-dependent uniaxial stress and strain can be expressed as a convolution integral of the following form.

$$\varepsilon(t) = \int_{-\infty}^{\infty} D(t-\tau)\frac{\partial \sigma(\tau)}{\partial \tau} d\tau \qquad [1]$$

where $\sigma(t)$, $\varepsilon(t)$, and $D(t)$ are the time-dependent stress, strain, and creep compliance, respectively. The above convolution equation can also be written as the following, known as the Riemann-Stieltjes integral (*6*):

$$\varepsilon(t) = D(0)\cdot\sigma(t) - \int_0^t \sigma(\tau)\frac{\partial}{\partial\tau}D(t-\tau)d\tau \qquad [2]$$

Following Lee and Kim (*5*), the above equation can be evaluated numerically for each given time step, t_n, as follows:

$$\varepsilon(t_n) = D(0)\cdot\sigma_n + \sum_{i=1}^{n-1}\left[\sigma_i\cdot\left\{D(t_n - t_i) - D(t_n - t_{i+1})\right\}\right], \quad \text{for } t_n = t_1 \ldots t_N \qquad [3]$$

where $\sigma_i = \sigma(\tau)$ for the discrete time interval $t_i < \tau < t_{i+1}$. Note that the above equation can be applied to any arbitrary functions $D(t)$ and $\sigma(t)$ that are numerically available.

4.2 Backcalculation of Creep Compliance Using Least Squares

In order to backcalculate the creep compliance using the least squares approach, it is necessary to identify a function that represents the creep compliance of viscoelastic materials. For this purpose, the power function, which has been well accepted as an analytical representation of the creep compliance of viscoelastic materials (*7*, *8*, *9*, *10*, *11*), has been selected due to its simple form. The function is expressed as:

$$D(t) = D_0 + D_1\cdot t^m \qquad [4]$$

The following equation is obtained by substituting Equation (4) into Equation (3):

$$\varepsilon(t_n) = D_0\cdot\sigma_n + D_1\cdot\sum_{i=1}^{n-1}\left[\sigma_i\cdot\left\{(t_n - t_i)^m - (t_n - t_{i+1})^m\right\}\right], \quad \text{for } t_n = t_1 \ldots t_N \qquad [5]$$

which can be used to calculate the time-dependent strain of a viscoelastic material with the $D(t)$ shown in Equation (4) subjected to any arbitrary loading $\sigma(t)$.

In order to determine the power function parameters D_0, D_1, and m from the strain output due to an arbitrary stress input using the least squares approach, the objective function is set up as follows:

$$F = \sum_{n=1}^{N} \left\{ \varepsilon(t_n) - \varepsilon_{m,n} \right\}^2 = \sum_{n=1}^{N} \left\{ D_0 \sigma_n + D_1 \xi_n - \varepsilon_{m,n} \right\}^2 \qquad [6]$$

where F is the function to be minimized, $\varepsilon_{m,n}$ is the measured strain at time $t = t_n$, and

$$\xi_n = \sum_{i=1}^{n-1} \left[\sigma_i \cdot \left\{ (t_n - t_i)^m - (t_n - t_{i+1})^m \right\} \right] \qquad [7]$$

Note that the objective function shown in Equation (6) leads to a non-linear least squares problem due to the parameter m in Equation (7). In order to overcome this difficulty, the m value has been assumed for each iteration to simplify the problem into a linear least squares in which the only remaining unknowns become, D_0 and D_1. Then, for a given m value, the function F is minimized when its partial derivative with respect to D_0 and D_1 equal to zero. This formulation results in a set of linear equations that can be expressed in the following matrix form:

$$\begin{Bmatrix} D_0 \\ D_1 \end{Bmatrix} = \begin{bmatrix} \sum_{n=1}^{N} \sigma_n{}^2 & \sum_{n=1}^{N} \sigma_n \xi_n \\ \sum_{n=1}^{N} \sigma_n \xi_n & \sum_{n=1}^{N} \xi_n{}^2 \end{bmatrix}^{-1} \begin{Bmatrix} \sum_{n=1}^{N} \varepsilon_{m,n} \sigma_n \\ \sum_{n=1}^{N} \varepsilon_{m,n} \xi_n \end{Bmatrix} \qquad [8]$$

5 REVIEW OF BACKCALCULATION METHODOLOGY FOR INDIRECT TENSION TESTING CONDITIONS

5.1 Elastic Stress Analysis for Indirect Tensile Test

The illustration of the IDT test and the plane-stress distribution within an IDT sample are shown schematically in Figure 1. For an IDT specimen with radius *R* and thickness *d* subjected to a strip load of width $a = 2R \cdot \sin(\alpha)$ and magnitude *P*, the distributions of the tensile stress along the horizontal axis and the compressive stress along the vertical axis were given by Hondros (*12*) under the assumption of plane-stress condition as:

$$\sigma_x(x,0) = \frac{2P}{\pi a d}\left[\frac{1-(x/R)^2\sin 2\alpha}{1+2(x/R)^2\cos 2\alpha+(x/R)^4} - \tan^{-1}\left(\frac{1-(x/R)^2}{1+(x/R)^2}\tan\alpha\right)\right] = \frac{2P}{\pi a d}m(x) \quad [9\text{-}1]$$

$$\sigma_y(0,y) = -\frac{2P}{\pi a d}\left[\frac{1-(y/R)^2\sin 2\alpha}{1-2(y/R)^2\cos 2\alpha+(y/R)^4} + \tan^{-1}\left(\frac{1+(y/R)^2}{1-(y/R)^2}\tan\alpha\right)\right] = -\frac{2P}{\pi a d}n(y) \quad [9\text{-}2]$$

from which the average stresses over the gauge length, *l*, are calculated as:

$$\sigma_{x,avg} = \frac{2P}{\pi a d}\cdot\frac{1}{l}\int_{-l/2}^{l/2} m(x)dx \quad [10\text{-}1]$$

$$\sigma_{y,avg} = -\frac{2P}{\pi a d}\cdot\frac{1}{l}\int_{-l/2}^{l/2} n(y)dy \quad [10\text{-}2]$$

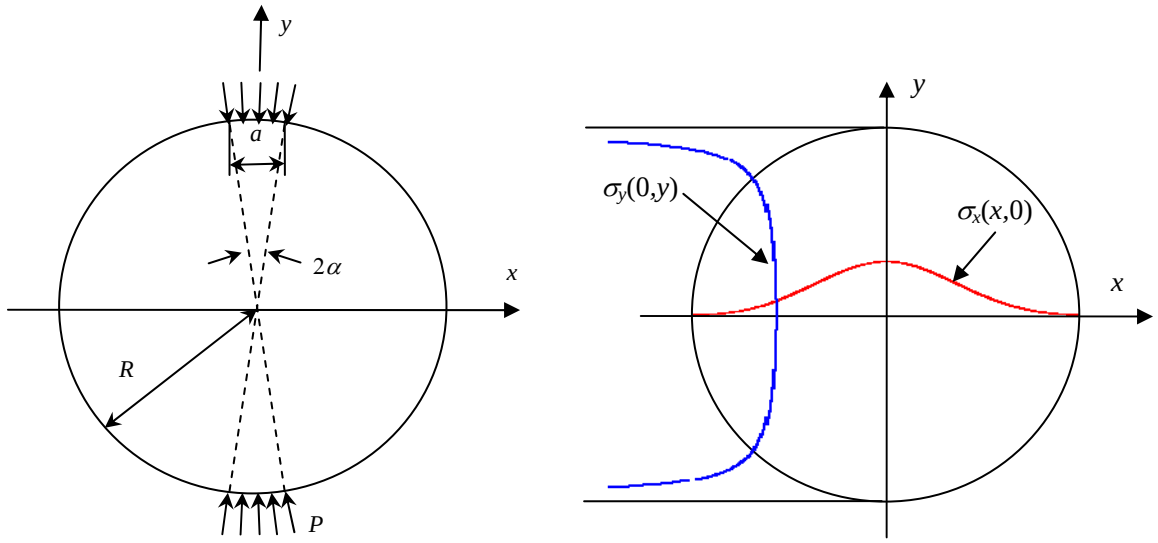

(a) (b)

Figure 1. (a) Schematic illustration of the IDT test and (b) plane stress distributions

Because of the nature of the IDT specimen geometry, another constant can be derived. This constant, β, is defined as the ratio of the horizontal and vertical stress magnitudes and is used to simplify the equations for the creep compliance formulation in IDT (*5*, *13*, *14*):

$$\beta = -\frac{\sigma_{y,avg}}{\sigma_{x,avg}} = \frac{\int_{-l/2}^{l/2} n(y)dx}{\int_{-l/2}^{l/2} m(x)dy} \quad [11]$$

For simplicity, the average horizontal and vertical stresses will be designated respectively as σ_x and σ_y in the subsequent sections of the paper.

5.2 Determining the Creep Compliance from Random Loading in the IDT Test

The plane-stress constitutive equations for a linear, elastic, and isotropic material are given as:

$$\varepsilon_x = D \cdot \left[\sigma_x - \mu\sigma_y\right] \quad [12\text{-}1]$$

$$\varepsilon_y = D \cdot \left[\sigma_y - \mu\sigma_x\right] \qquad [12\text{-}2]$$

where D and μ are the elastic compliance and Poisson's ratio for the given material, respectively. According to the elastic-viscoelastic correspondence principle, the constitutive equations for a viscoelastic material in the Laplace domain are obtained by replacing the elastic material properties with their viscoelastic counterparts multiplied by the Laplace variable (*6*, *7*, *15*). Therefore, the plane-stress constitutive equations for a viscoelastic material are given as:

$$\hat{\varepsilon}_x(s) = s\hat{D}(s)\cdot\left[\hat{\sigma}_x(s) - s\hat{\mu}(s)\hat{\sigma}_y(s)\right] \qquad [13\text{-}1]$$

$$\hat{\varepsilon}_y(s) = s\hat{D}(s)\cdot\left[\hat{\sigma}_y(s) - s\hat{\mu}(s)\hat{\sigma}_x(s)\right] \qquad [13\text{-}2]$$

where $L[f(t)] = \hat{f}(s) = \int_0^\infty e^{-st} f(t)dt$ is the Laplace transform of the function $f(t)$, s is the Laplace variable, and $\hat{D}(s)$ and $\hat{\mu}(s)$ are the Laplace transformed creep compliance and Poisson's ratio, respectively. Rearranging the terms after eliminating $\hat{\mu}(s)$ from Equations (13-1) and (13-2), and taking the inverse Laplace transform yields:

$$\left\{\varepsilon_x(t) + \beta\varepsilon_y(t)\right\} = \int_{0^-}^{t} D(t-\tau)\frac{\partial}{\partial\tau}\left\{\sigma_x(\tau) + \beta\sigma_y(\tau)\right\}d\tau \qquad [14]$$

where β was defined in Equation (11). The above equation is essentially identical to Equation (1) if the following substitutions are made for the stress, $\sigma(t)$, and strain, $\varepsilon(t)$, terms in Equation (1):

$$\varepsilon(t) = \left\{\varepsilon_x(t) + \beta\varepsilon_y(t)\right\} \qquad [15]$$

$$\sigma(t) = \left\{\sigma_x(t) + \beta\sigma_y(t)\right\} \qquad [16]$$

Then, with the above replacement of variables and the power function shown in Equation (4) for creep compliance, the same derivation and numerical scheme outlined for the uniaxial case

(Equations (1) through (8)) can be followed to backcalculate the creep compliance for the biaxial loading conditions. By using the direct search method for the *m* value, the remaining power function parameters D_0 and D_1 can be determined from the following:

$$\begin{Bmatrix} D_0 \\ D_1 \end{Bmatrix} = \begin{bmatrix} \sum_{n=1}^{N}\left(\sigma_{x,n} + \beta\sigma_{y,n}\right)^2 & \sum_{n=1}^{N}\left(\sigma_{x,n} + \beta\sigma_{y,n}\right)\xi_n \\ \sum_{n=1}^{N}\left(\sigma_{x,n} + \beta\sigma_{y,n}\right)\xi_n & \sum_{n=1}^{N}\xi_n{}^2 \end{bmatrix}^{-1} \begin{Bmatrix} \sum_{n=1}^{N}\left(\varepsilon_{x,n} + \beta\varepsilon_{y,n}\right)\left(\sigma_{x,n} + \beta\sigma_{y,n}\right) \\ \sum_{n=1}^{N}\left(\varepsilon_{x,n} + \beta\varepsilon_{y,n}\right)\xi_n \end{Bmatrix} \quad [17]$$

where

$$\xi_n = \sum_{i=1}^{n-1}\left[\left(\sigma_{x,i} + \beta\sigma_{y,i}\right)\cdot\left\{\left(t_n - t_i\right)^m - \left(t_n - t_{i+1}\right)^m\right\}\right] \quad [18]$$

6 CONVERSION OF CREEP COMPLIANCE TO DYNAMIC MODULUS

Although the power function has been successfully used for representing the creep behavior of viscoelastic materials, its mathematical deficiency does not provide enough flexibility for analytical interconversion of the fundamental properties of viscoelastic media. Instead, the Prony series has been widely used for the purpose of interconversion because of its mathematical efficiency. For creep compliance in the time domain, the Prony series representation takes the following form:

$$D(t) = D_0^p + \sum_{i=1}^{M} D_i^p\left(1 - e^{-\frac{t}{\tau_i}}\right) \quad [19]$$

where D_0^p, and D_i^p, are the Prony series parameters, and τ_i are the retardation times. In fitting creep compliances using the Prony series, the retardation times, τ_i, are usually specified, and then the unknown coefficients are determined by solving the linear system of equations (*11*, *16*). In this study, the Prony series shown in Equation (19) was fitted to the backcalculated creep compliance, expressed in terms of the power function, with *M*=7 and retardation times of one decade interval, $\tau_i = 10^{(i-4)}$ (i = 1,… 7).

Once the Prony series parameters have been determined, the real (*D'*) and imaginary (*D"*) parts of the complex compliance can be obtained by (*5*, *15*, *17*):

$$D'(\omega) = D_0^p + \sum_{i=1}^{M} \frac{D_i^p}{\omega^2 \tau_i^{\,2} + 1} \qquad [20]$$

$$D''(\omega) = \sum_{i=1}^{M} \frac{\omega \tau_i D_i^p}{\omega^2 \tau_i^{\,2} + 1} \qquad [21]$$

where ω is the angular frequency. Then, the dynamic modulus is obtained as the reciprocal of the complex compliance as shown in the equation below:

$$\left|E^*(\omega)\right| = \frac{1}{\left|D^*(\omega)\right|} = \frac{1}{\sqrt{D'(\omega)^2 + D''(\omega)^2}} \qquad [22]$$

7 EXPERIMENTAL STUDY USING LABORATORY-COMPACTED MIXTURES

In order to evaluate the usefulness and effectiveness of the backcalculation algorithm, laboratory experiments have been conducted in both the uniaxial compressive mode and indirect tension (IDT) mode. The material selected for testing was a dense graded asphalt mixture meeting all Superpave requirements. The material was sampled from a local plant and compacted in the

laboratory. The mixture included 15 percent Reclaimed Asphalt Pavement (RAP), a 12.5 mm nominal aggregate size, a PG76-22 modified binder, and a total binder content of 5.2 percent. The volumetric properties of the mixture are summarized in Table 1.

Table 1. Volumetric properties of the laboratory-fabricated mixture

Sieve Size / Mixture Property	Percent Passing / Property Value
19 mm	100
12.5 mm	99
9.5 mm	90
# 4	64
# 8	42
# 16	30
# 30	22
# 50	13
# 100	6
# 200	4
Specific Gravity for Aggregates, G_{sb}	2.647
Specific Gravity for Mixture, G_{mm}	2.494
Total Asphalt Content, P_b	5.2 %
RAP Asphalt Content	0.9 %
Virgin Asphalt Content	4.3 %

7.1 Specimen Preparation

For uniaxial compression testing, three replicate specimens 170 mm tall by 150 mm in diameter were prepared with a Superpave Gyratory Compactor. These gyratory specimens were cored and trimmed to a final size of 150 mm tall by 100 mm in diameter in accordance with AASHTO TP 62. For IDT testing, test specimens 185 mm tall by 150 mm in diameter were prepared with the same Superpave Gyratory Compactor. From each specimen, three replicates of 38 mm thick IDT samples were carefully cut from the middle of the specimen. All the uniaxial and IDT samples met the 7 percent target air void with a tolerance of ± 0.5 percent in accordance with AASHTO T 322.

7.2 Uniaxial and IDT Testing on Mixtures

The uniaxial compressive testing, which is the primary testing mode in the MEPDG, is normally conducted in the intermediate to high temperature range (approximately 0°C to 60°C), while the

IDT, which has been used for evaluating the resilient modulus, creep, and tensile strength (*8*, *18*, *19*) of asphalt mixtures, is conducted in the low to intermediate temperature range (approximately -30°C to 30°C). Therefore, it was decided to conduct the uniaxial testing at 0°C, 10°C, 20°C, and 40°C and the IDT testing at 0°C, 10°C, 20°C, and 30°C.

A picture of the uniaxial test setup with specimen dimensions is shown in Figure 2. For the uniaxial test, resilient modulus tests followed by dynamic modulus and by creep tests were all performed in the compression mode. The resilient modulus test was conducted for five cycles in which each cycle consisted of a 0.1-second haversine load followed by a 0.9-second rest period. The data were measured according to the method documented in a previous study (*8*). Then, the dynamic modulus tests were conducted at frequencies of 0.1 Hz, 0.5 Hz, 1.0 Hz, 5.0 Hz, and 10.0 Hz, with rest periods of at least five minutes between the individual tests. Finally, the creep test was conducted for a duration of 1,000 seconds. All of the above tests conducted in the uniaxial mode were also repeated in the IDT mode. A picture of the IDT specimen and the testing setup is shown in Figure 3. The system for measuring the stress and strain responses was in accordance with AASHTO T 322. The maximum strain in the resilient modulus test performed under the uniaxial testing mode and the maximum horizontal strain in the same test under the IDT testing mode were kept below 100 με.

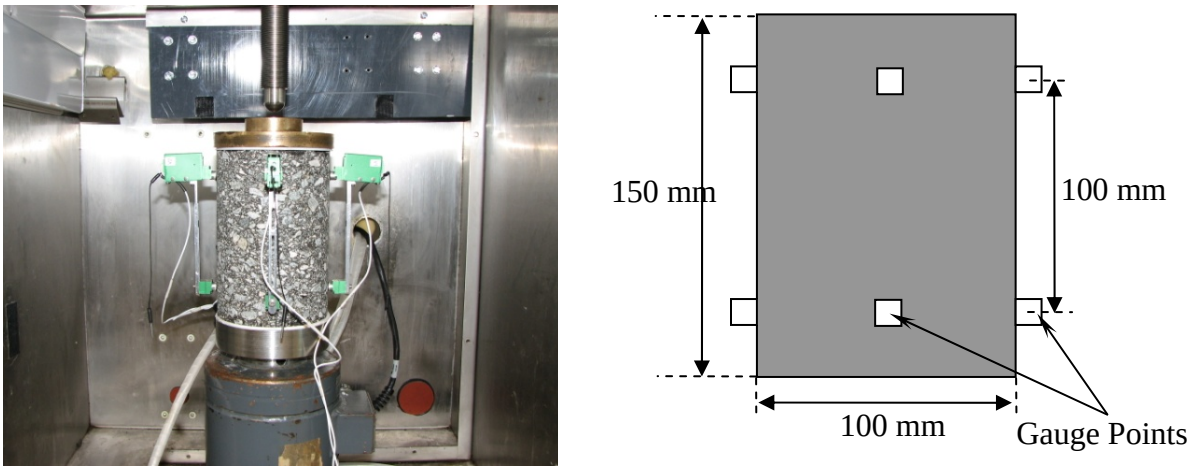

(a) (b)

Figure 2. (a) Uniaxial test setup and (b) specimen dimensions

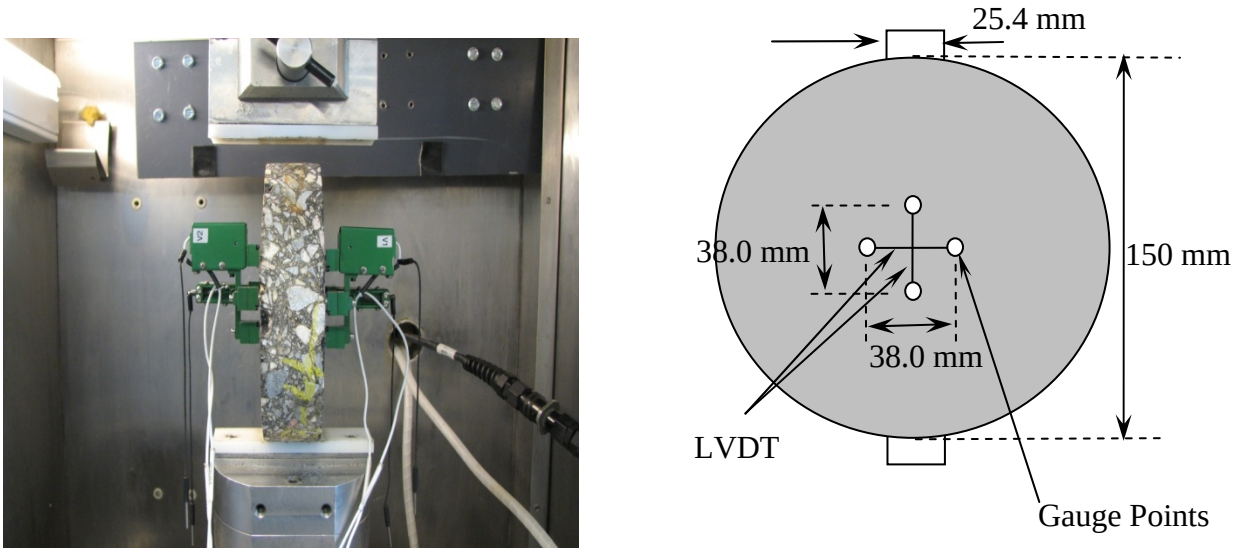

(a) (b)

Figure 3. (a) Indirect tensile test setup and (b) specimen dimensions

7.3 Comparison of Dynamic Modulus Master Curves from Indirect Tensile and Uniaxial Test Modes

The uniaxial compressive testing has been chosen by the MEPDG as the standard testing mode for evaluation of the asphalt dynamic modulus and construction of the master curve. However, obtaining a field core meeting the specimen size requirement for this testing mode could pose some challenges. As an example, a recent research funded by FDOT indicated that out of 25 in-service pavement sections studied as part of FDOT's efforts to implement the MEPDG, only 6 test sections had a total asphalt thickness in excess of 150 mm, suitable for carrying out the dynamic modulus tests in the uniaxial compression mode (*20*). It should also be noted that the asphalt layer in Florida is typically constructed with multiple lifts of thickness ranging from 40 mm to 50 mm. For this reason, the uniaxial testing conducted on field asphalt cores can only represent the behavior of the composite asphalt mat which may be composed of layers with different age, gradation, binder content, etc. Due to these reasons, the majority of FDOT's previous tests conducted on field cores had been carried out in the IDT mode rather than in the uniaxial mode. Therefore, a quick comparison of results from the uniaxial and IDT test modes are shown in this section of the paper to evaluate the feasibility of the IDT dynamic modulus as input into the new design guide. It should be noted that the comparisons are limited to those

from the dynamic modulus testing. The backcalculation results will be presented in subsequent sections of the paper.

The dynamic modulus from the uniaxial test was obtained according to the procedures outlined in AASHTO TP 62. The procedure for obtaining the dynamic modulus in the IDT mode is briefly described herein. Detailed mathematical derivations can be found in Lee and Kim (*5*).

From the plane-stress constitutive equation for a linear elastic material shown in Equation (12), the constitutive equation for a viscoelastic material in the frequency domain can be obtained by replacing *D* and μ in Equation (12) by their viscoelastic counterparts (*7*, *15*):

$$\varepsilon_x^* = D^* \cdot \left[\sigma_x^0 - \mu^* \sigma_y^0\right] \quad [23\text{-}1]$$

$$\varepsilon_y^* = D^* \cdot \left[\sigma_y^0 - \mu^* \sigma_x^0\right] \quad [23\text{-}2]$$

where ε_x^* and ε_y^* are the complex amplitudes of the horizontal and vertical strains, σ_x^0 and σ_y^0 are the horizontal and vertical stress amplitudes, and D^* and μ^* are the viscoelastic, complex compliance and Poisson's ratio, respectively. Combining Equations (23-1), (23-2), and (11) by eliminating μ^* yields a single equation for D^*:

$$D^*(\omega) = \frac{\varepsilon_x^* + \beta\varepsilon_y^*}{\sigma_x^0 + \beta\sigma_y^0} \quad [24]$$

As already mentioned, taking the reciprocal of the dynamic compliance, |*D**|, obtained from the above equation, results in the dynamic modulus, |*E**|, in the IDT testing mode. For simplicity, the dynamic modulus obtained from the dynamic modulus tests will be referred to as the "measured" dynamic modulus in the remaining sections of the paper.

As mentioned earlier, both the uniaxial and the IDT dynamic modulus tests were conducted at 4 distinct temperatures among which 3 temperatures (0ºC, 10ºC, and 20ºC) were common in both

the uniaxial and IDT mode. Figure 4 shows a comparison of the dynamic modulus values measured in the uniaxial and IDT mode at the 3 temperatures mentioned above and at 5 different frequencies (0.1 Hz, 0.5 Hz, 1.0 Hz, 5.0 Hz, and 10.0 Hz). The figure shows that the measured dynamic moduli from the uniaxial and those from the IDT modes are in good agreement, with an R^2 value of 0.98. The figure also shows that the IDT dynamic modulus values are slightly greater than those from the uniaxial test. Although this was not expected, it should be noted that the average absolute percent error between the two test modes was 8.7 percent which is less than the estimated accuracy limit of the test method (approximately 12 to 13 percent) reported in AASHTO TP 62. Therefore, similar to a previous study conducted by Kim et al. (*21*), it can be concluded that the dynamic modulus measured in the IDT mode is a reasonable estimate of the dynamic modulus measured in the uniaxial mode.

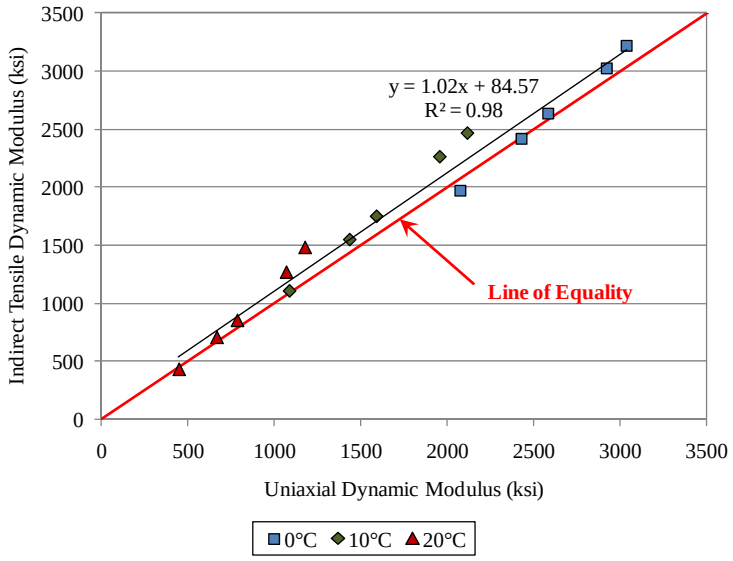

Figure 4. Comparison of Measured Uniaxial and IDT Dynamic Modulus

7.4 Generation of Master Curve Using Backcalculated Dynamic Modulus

Using the methodology presented earlier in the paper, the power function parameters for the creep compliance were backcalculated from the resilient modulus test data. Then, the Prony series was fitted to the creep compliance and was used to convert the creep compliance to the dynamic modulus values corresponding to the same frequencies at which the actual dynamic modulus tests were conducted (0.1 Hz, 0.5 Hz, 1.0 Hz, 5.0 Hz, and 10.0 Hz). Figure 5 shows a comparison between the measured and the backcalculated dynamic modulus for both the uniaxial

and IDT mode. The average absolute percent errors between the measured and the backcalculated dynamic moduli were calculated to be 9.9 and 10.7 percent for the uniaxial and IDT test modes, respectively. Since these errors were less than the estimated limit of accuracy, the master curves were constructed using both the measured and backcalculated dynamic modulus values. All of the master curves presented in this paper were generated for a reference temperature of 10°C.

Figures 6 and 7 show the master curves constructed using measured and backcalculated dynamic moduli, for the uniaxial and IDT testing mode, respectively. For clarity, the master curves are shown in both arithmetic and logarithmic scales. It can be seen from the figures that regardless of the testing mode, the master curve from the backcalculated dynamic modulus has reasonable agreement with the master curve from the measured modulus at higher frequencies (or equivalently lower temperatures), but they tend to deviate from each other at lower frequencies (or higher temperatures). It was also found that this was more pronounced in the uniaxial mode than in the IDT mode. The authors believe that this is mainly caused by the combined effect of the following: (1) the fast rate of loading (0.1 sec. for loading and unloading with a rest period of 0.9 sec.) and the short duration (5 sec.) of the resilient modulus test not being able to disclose the prominent viscoelastic behavior of the material at elevated temperatures and low frequencies that are equivalent to the long time range in the physical time domain, (2) the backcalculated frequency range (0.1 Hz to 10.0 Hz) not being wide enough to provide sufficient overlap of the dynamic modulus between successive temperatures, and (3) the inevitable errors associated with the backcalculation. As explained by Kim et al. (*21*), sufficient overlap of modulus values in successive testing temperatures is one of the most important requirements in construction of the master curve. A closer look at Figure 5 (a) indicates that there is not a significant overlap of modulus between different test temperatures.

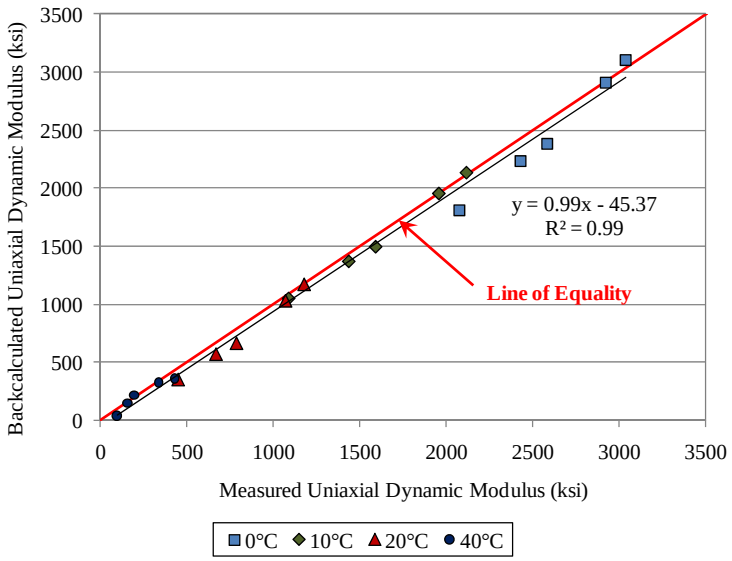

(a)

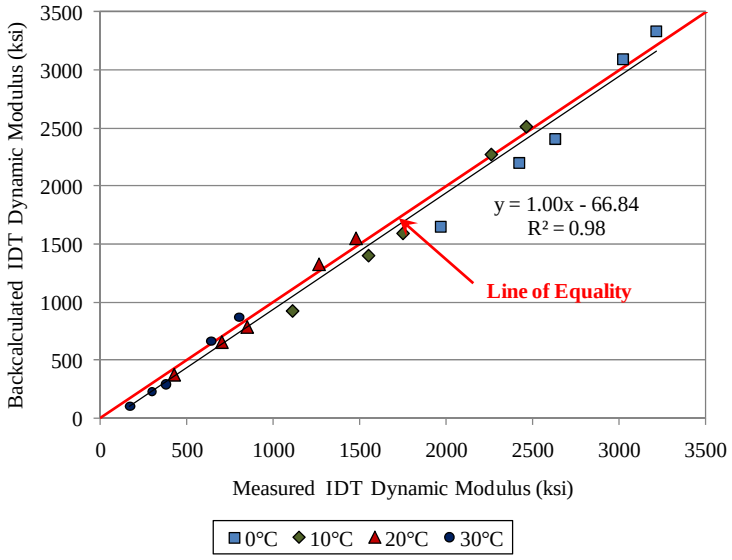

(b)

Figure 5. Measured vs. Backcalculated (from Resilient Modulus) in (a) Uniaxial and (b) IDT test modes

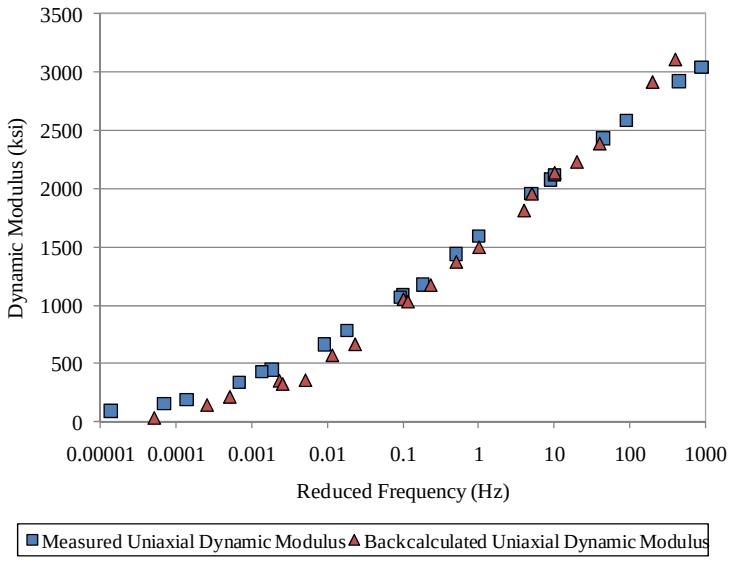

(a)

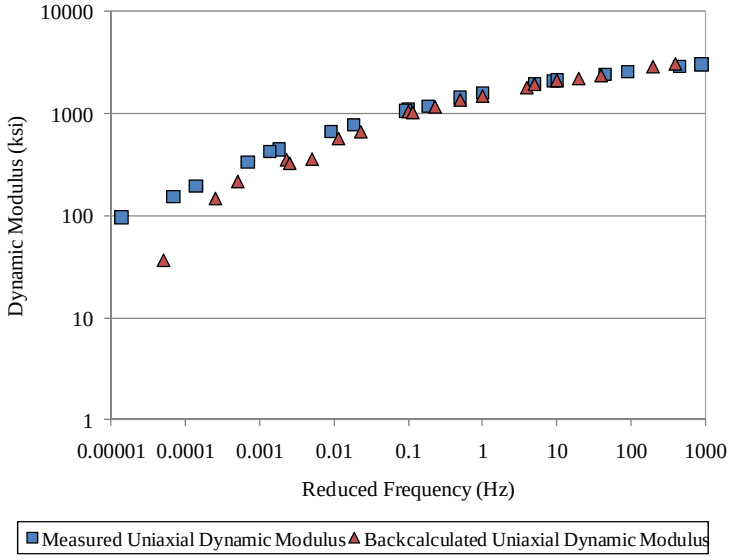

(b)

Figure 6. Master Curves at 10°C from Measured vs. Backcalculated (from Resilient Modulus Test) Uniaxial Dynamic Moduli in (a) Arithmetic and (b) Logarithmic Scales

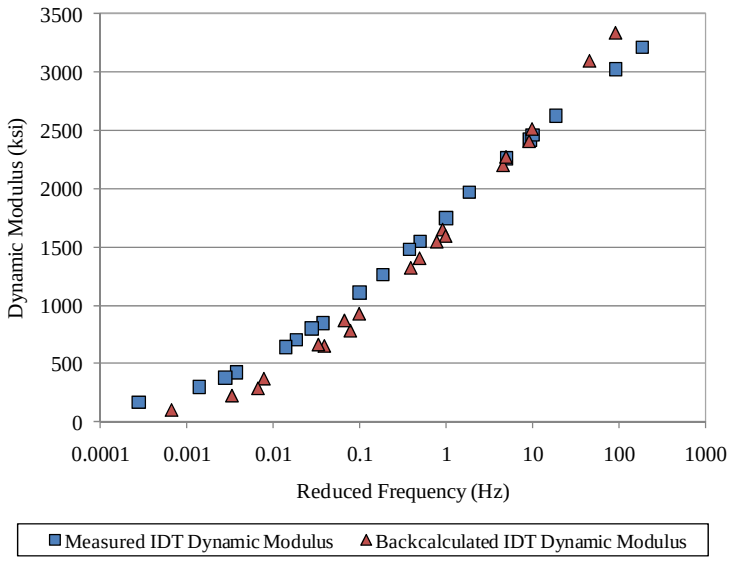

(a)

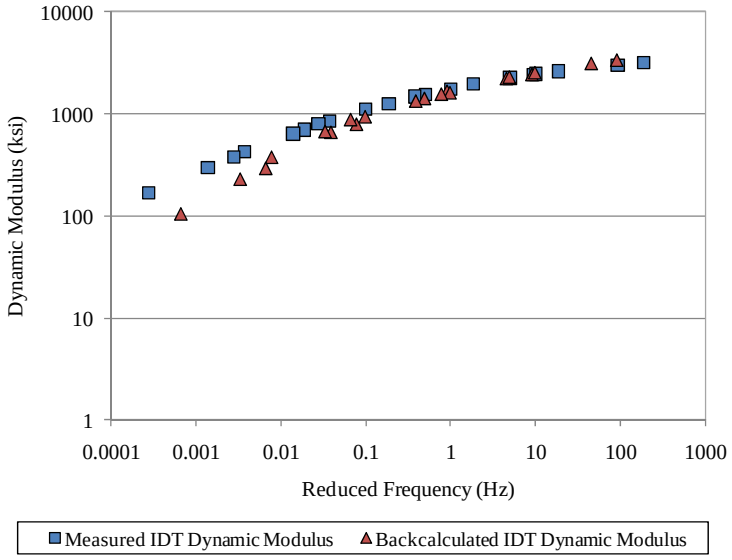

(b)

Figure 7. Master Curves at 10°C from Measured vs. Backcalculated (from Resilient Modulus Test) IDT Dynamic Moduli in (a) Arithmetic and (b) Logarithmic Scales

Based on the above reasoning, it was hypothesized that the backcalculated creep compliance (and hence the dynamic modulus) at higher temperatures and lower frequencies (or longer time range) could be enhanced by using the creep test data for the same mixture. As per

AASHTO T 322, FDOT typically conducts the creep test for a duration of 1,000 seconds and hence, it is believed to give a better estimate of the viscoelastic properties for a longer time range than the backcalculated properties from the 5 second resilient modulus test. In addition, because the creep test is conducted for a long duration (compared to the resilient modulus test), it was hypothesized that incorporation of the creep test data may allow for estimating the dynamic modulus at a wider range of frequency.

7.5 Enhancing the Backcalculated Dynamic Modulus by Means of Creep Test Data

The idea behind the methodology presented in here was first proposed by Kim et. al. (*11*), who showed that the creep compliance obtained from dynamic modulus testing at a single temperature and limited frequencies (0.1 Hz to 25.0 Hz) was a better representation of the material behavior at short loading times (or equivalently higher frequencies), whereas the creep compliance from the actual creep test represented the material behavior at long loading times (or equivalently lower frequencies). The creep compliances obtained from both the creep and dynamic modulus tests were combined through the use of Prony series to obtain an enhanced creep compliance curve that is accurate in both the short and long time ranges. This was accomplished by replacing the last two terms of the Prony series (shown in Equation (19)) calculated from the dynamic modulus test data with the ones obtained from the creep test. The enhanced creep compliance was also verified through an experimental study where the sample was subject to a cyclic loading of over 300 cycles. The same methodology described above was used in this study to enhance the creep compliance and the dynamic modulus estimated at each temperature. The only obvious difference is that the creep data was used to enhance the backcalculated dynamic modulus (rather than the measured dynamic modulus) especially at lower frequencies.

Figure 8 shows the comparison between the measured dynamic modulus and the backcalculated dynamic modulus enhanced with creep data, for the range of frequency used in the dynamic modulus testing (0.1 Hz to 10.0 Hz). Comparing Figure 8 with Figure 5, it can be observed that the slopes of the linear regression line had negligible change and the magnitudes of the y-intercept in both figures had slightly decreased, indicating that the regression line moved closer to the line of equality after the enhancement. After the enhancement, the average absolute

percent errors between the measured and backcalculated dynamic moduli were determined to be 10.1 and 10.2 percent for the uniaxial and IDT test modes, respectively, and were both below the estimated limit of accuracy. The percent error for the uniaxial test mode increased by 0.2 percent, which was considered to be negligible for all practical purposes.

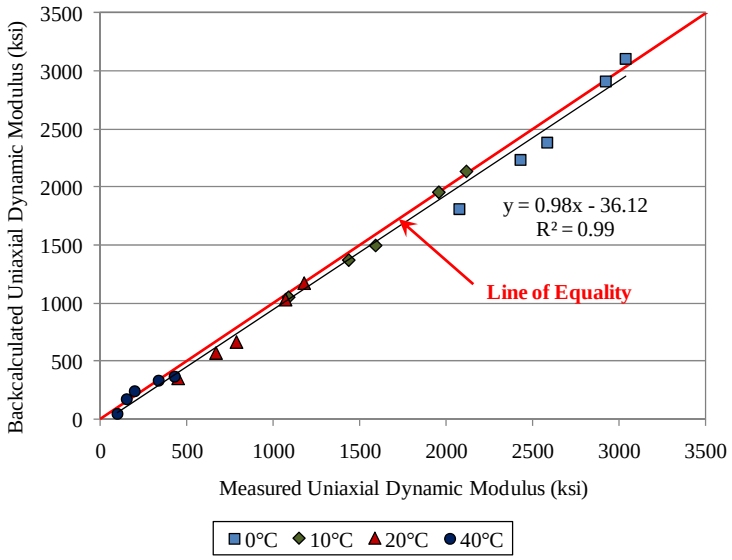

(a)

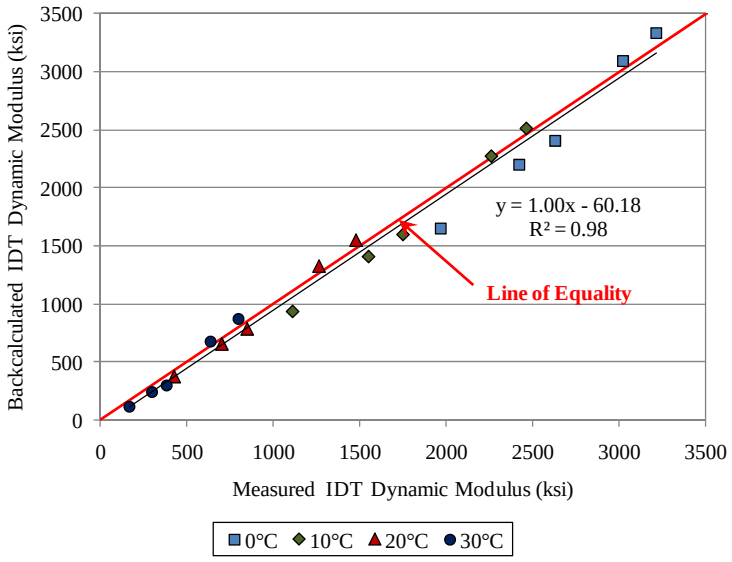

(b)

Figure 8. Measured vs. Backcalculated (from Resilient Modulus and Creep) in (a) Uniaxial and (b) IDT test modes

As it was briefly mentioned, another potential and possibly more crucial advantage of enhancing the backcalculated dynamic modulus using the creep data is that since the creep test was conducted for 1,000 seconds, it allows for estimating the dynamic modulus at frequencies lower than the lowest frequency at which the actual dynamic modulus tests were conducted (0.1 Hz). Therefore, the enhanced creep compliance was converted to the dynamic modulus at 0.005 Hz, 0.01 Hz, and 0.05 Hz, in addition to all frequencies where the actual dynamic modulus test was conducted (0.1 Hz to 10.0 Hz). The master curves from the enhanced dynamic modulus have been constructed by taking these additional frequencies into account to allow for some overlap of the modulus values between the different temperatures. The updated master curves are shown in Figures 9 and 10, for the uniaxial and IDT modes, respectively, along with the master curves from the measured dynamic modulus. Figure 11 shows the shift factors that were calculated in obtaining the different master curves. Compared to those shown in Figures 6 and 7, the backcalculated master curves shown in Figures 9 and 10 show better agreement with those from the measured dynamic modulus especially at lower frequencies. This clearly illustrates the advantage of enhancing the creep compliance and hence the backcalculated dynamic modulus using the creep test data.

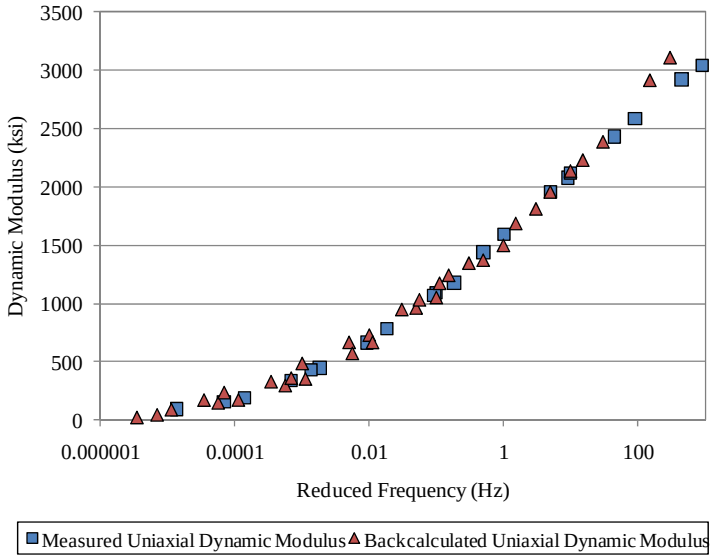

(a)

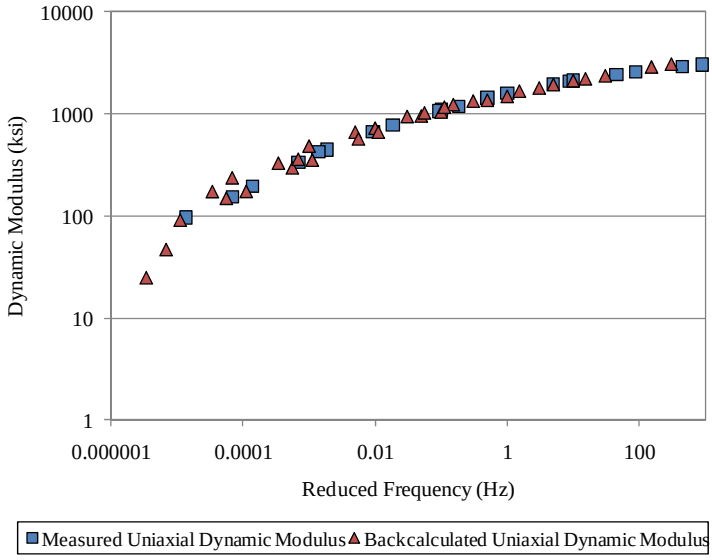

(b)

Figure 9. Master Curves at 10°C from Measured vs. Backcalculated (from Resilient Modulus and Creep Tests) Uniaxial Dynamic Moduli in (a) Arithmetic and (b) Logarithmic Scales

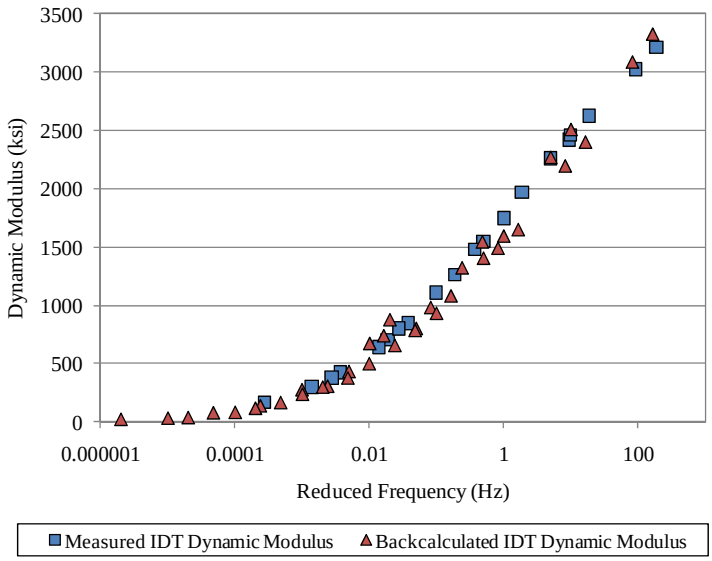

(a)

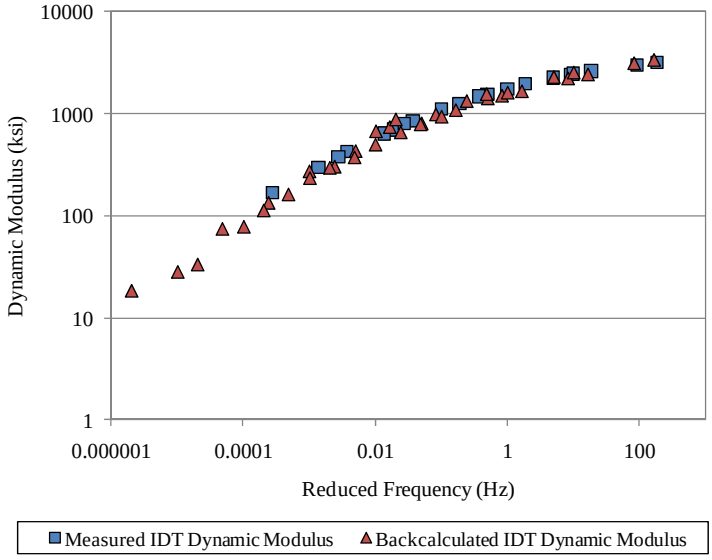

(b)

Figure 10. Master Curves at 10°C from Measured vs. Backcalculated (from Resilient Modulus and Creep Tests) IDT Dynamic Moduli in (a) Arithmetic and (b) Logarithmic Scales

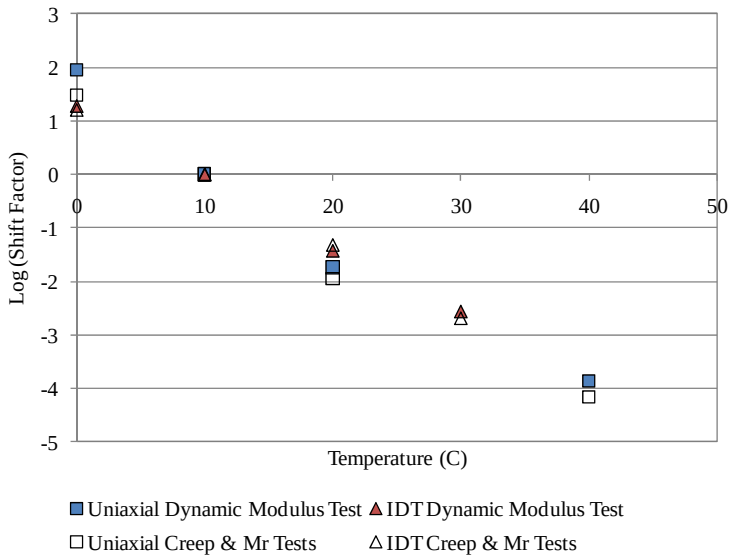

Figure 11. Shift Factors for Constructing the Master Curves

8 SUMMARY AND CONCLUSIONS

Because of the difficulty associated with the dynamic modulus test in the uniaxial mode, FDOT has been conducting most of their testing on field cores in the IDT mode. In addition, because the dynamic modulus is not required in calculating the Energy Ratio of the tested mixture, the dynamic modulus tests were not typically conducted in previous research studies. Instead, FDOT primarily conducted the Superpave IDT tests, namely resilient modulus, creep, and strength tests, on the IDT specimens. In order to allow for the historical IDT test data to be used in the new design guide, a methodology was necessary to estimate the dynamic modulus and to construct the dynamic modulus master curve from the above tests.

In this study, a methodology was presented that allows for backcalculating the fundamental viscoelastic material property, that is, creep compliance from the random loading and its corresponding response. The creep compliance in terms of the power function was backcalculated from the commonly used uniaxial and IDT resilient modulus test data using the algorithms derived from the viscoelastic constitutive relations. Then, the dynamic modulus master curves were generated from the measured and backcalculated dynamic modulus values.

Although the master curve from the backcalculated dynamic modulus showed reasonable agreement with those from the measured dynamic modulus, deviations were noticed in the lower frequency (or higher temperature) ranges. In order to overcome this problem, the backcalculated dynamic modulus was enhanced using the creep test data. The master curves generated using these enhanced dynamic modulus showed a better agreement with those from the measured dynamic modulus.

Although the Mechanistic-Empirical Pavement Design Guide (MEPDG) could not endorse the use of the resilient modulus test protocol as the primary means of asphalt concrete modulus characterization in the design of flexible pavements, it has been a primary mixture test, and a considerable amount of laboratory testing has been done to date**.** The practical nature of the proposed backcalculation methodology coupled with the approach developed in this study would allow for evaluating the dynamic modulus of asphalt mixtures from existing resilient modulus and creep test data, and the construction of the master curves for input into the new design guide.

9 ACKNOWLEDGEMENTS

The authors would like to acknowledge James Greene, Gregory Sholar, Charles Holzschuher, Patrick Upshaw, Kenneth Green, and Sandy Mihocik for their diligent efforts and invaluable recommendations provided throughout the duration of the research.

10 REFERENCES

1. American Association of State Highway and Transportation Officials. *AASHTO Guide for Design of Pavement Structures*. American Association of State Highway and Transportation Officials, Washington, D.C., U.S.A. 1993.
2. Roque, R., B. Birgisson, C. Drakos, and B. Dietrich. Development and field evaluation of energy-based criteria for top-down cracking performance of hot mix asphalt. *Journal of the Association of Asphalt Paving Technologists*, Vo. 73, 2004. pp. 229-260.
3. Zhang, Z., R. Roque, B. Birgisson, and B. Sangpetgnam. Identification and Verification of a Suitable Crack Growth Law for Asphalt Mixtures. *Journal of the Association of Asphalt Paving Technologists*, Vo. 70, 2001. pp. 206-241.
4. ARA., ERES Division. *Guide for Mechanistic-Empirical Design of New and Rehabilitated Pavement Structures*. National Cooperative Highway Research Program1-37A, Transportation Research Board, National Research Council. 2004.
5. Lee, H. S., and J. Kim. Backcalculation of Dynamic Modulus from Resilient Modulus Test Data. *Canadian Journal of Civil Engineering*, Vol. 38, No. 5, 2011. pp 582-592.
6. Wineman, A. S., and K. R. Rajagopal. *Mechanical response of polymers: An introduction*. Cambridge University Press, New York. 2000.
7. Findley, W. N., J. S. Lai, and K. Onaran. *Creep and relaxation of nonlinear viscoelastic materials*. Dover Publications, Inc., New York. 1976.
8. Roque, R., W. G. Buttlar, B. E. Ruth, M. Tia, S. W. Dickison, and B. Reid. Evaluation of SHRP indirect tension tester to mitigate cracking in asphalt concrete pavements and overlays. Final Report, FDOT B-9885, University of Florida, Gainesville, FL. 1997.
9. Roque, R., W. G. Buttlar, B. E. Ruth, and S. W. Dickison. Short-Loading-Time Stiffness from Creep, Resilient Modulus, and Strength Tests Using Superpave Indirect Tension Test. In *Transportation Research Record: Journal of the Transportation Research Board*, No. 1630, Transportation Research Board of the National Academies, Washington, D. C., 1998, pp. 10-20.

10. Kim, J., R. Roque, and B. Birgisson. Obtaining creep compliance parameters accurately from static or cyclic creep tests. *ASTM International*, ASTM STP, Vol. 1469, 2005.pp. 177-197.
11. Kim, J., G. Sholar, and S. Kim. Determination of accurate creep compliance and relaxation modulus at a single temperature for viscoelastic solids. *Journal of Materials in Civil Engineering*, ASCE, Vol. 20, No. 2, 2008. pp. 147-156.
12. Hondros, G. The evaluation of Poisson's ratio and the modulus of materials of a low tensile resistance by the brazilian (indirect tensile) test with particular reference to concrete. *Australian Journal of Applied Science*, Vol. 10, No. 3, 1959. pp. 243-268.
13. Lee, H. S., and J. Kim. Determination of viscoelastic Poisson's ratio and creep compliance from the indirect tension test. *Journal of Materials in Civil Engineering*, ASCE, Vol. 21, No. 8, 2009. pp 416-425.
14. Kim, J. and R. C. West. Application of the viscoelastic continuum damage model to the indirect tension test at a single temperature. *Journal of Engineering Mechanics*, ASCE, Vol. 136, No. 4, 2010. pp 496-505.
15. Kim, Y. R. *Modeling of Asphalt Concrete*. ASCE Press. McGraw Hill. 2009.
16. Park, S. W., and Y. R. Kim. Fitting prony-series viscoelastic models with power-law presmoothing. *Journal of Materials in Civil Engineering*, ASCE, Vol. 13, No. 1, 2001. pp. 26–32.
17. Park, S. W., and R. A. Schapery. Methods of interconversion between linear viscoelastic material functions. Part I – a numerical method based on Prony Series. *International Journal of Solids and Structures*, Vol. 36, 1999. pp 1653-1675.
18. Roque, R., and W. G. Buttlar. The development of a measurement and analysis system to accurately determine asphalt concrete properties using the indirect tensile mode. *Journal of the Association of Asphalt Paving Technologists*, Vol. 61, 1992. pp. 304-332.
19. Buttlar, W. G., and R. Roque. Development and evaluation of the strategic highway research program measurement and analysis system for indirect tensile testing at low temperatures. In *Transportation Research Record; Journal of the Transportation Research Board*, No. 1454, Transportation Research Board of the National Academies, Washington, D. C., 1994. pp. 163-171.

20. Oh, J. H. and E. Fernando. *Comparison of Resilient Modulus Values Used in Pavement Design*. Final Report, FDOT BDL76, Texas Transportation Institute, College Station, TX. 2011.
21. Kim, Y. R, Y. Seo, M. King, and M. Momen. Dynamic Modulus Testing of Asphalt Concrete in Indirect Tension Mode. In *Transportation Research Record: Journal of the Transportation Research Board*, No. 1891, Transportation Research Board of the National Academies, Washington, D. C., 2004, pp. 163-173.